

Phase equilibria and clustering in size-asymmetric primitive model electrolytes

Qiliang Yan and Juan J. de Pablo

Department of Chemical Engineering, University of Wisconsin-Madison, Madison, Wisconsin 53706

(Received 25 September 2000; accepted 24 October 2000)

The low-temperature phase coexistence of size-asymmetric primitive model electrolyte solutions has been investigated by means of Monte Carlo simulations. A multidimensional parallel tempering method is employed and results are analyzed by means of histogram reweighting. Coexistence curves and critical constants are determined as a function of size asymmetry, $\lambda = \sigma_+ / \sigma_-$, from 0.05 to 1. It is found that the critical temperature and the critical density decrease as λ decreases. These trends appear to contradict available integral-equation theoretical predictions. For highly asymmetric systems, we report the formation of large chain-like and ring-like structures. These clusters are much larger than those observed in symmetric electrolytes, and they are shown to give rise to considerable finite-size effects. © 2001 American Institute of Physics.

[DOI: 10.1063/1.1335653]

I. INTRODUCTION

Electrolyte solutions are often described in terms of primitive models (PM), where the system is represented by a binary mixture of charged hard spheres immersed in a dielectric continuum. Much of our understanding of electrolytes, including the seminal work of Debye and Hückel,¹ is based on such models.²⁻⁵ In the “restricted” primitive model (RPM), the anions and cations have the same charge and size. That model exhibits a vapor–liquid coexistence at low temperatures which has been the subject of considerable attention. Over the last few years, a number of molecular simulations have gradually determined the precise location of the coexistence curve and its critical temperature T_c and density ρ_c .⁶⁻⁸

Simulations of the phase behavior of the restricted primitive model have required development of new, increasingly powerful simulation methods. Given the associative nature of the model and the low temperature involved, such simulations require considerable computational resources. Not surprisingly, most theoretical work to date and all published simulation studies have been limited to the restricted primitive model. Real electrolytes, however, are generally asymmetric. Unfortunately, much less effort has been devoted to the study of the more general case of asymmetric systems.

This work provides a first attempt to investigate, by means of molecular simulations, the effects of size asymmetry on the phase behavior and critical properties of primitive models. The simulations presented here are performed in the context of a recently proposed hyperparallel tempering Monte Carlo method.⁶ The results of our simulations are compared to predictions of integral equation calculations using a mean spherical approximation (MSA). Our findings suggest that the general trends observed for T_c and ρ_c in simulations are in conflict with the MSA theory.⁹

Section II discusses the details of our simulations, including the models employed here and the hyperparallel tempering Monte Carlo method. In Sec. III we present the results

of our simulations and we compare these to theory. We close this paper with several remarks regarding the questions that have emerged as a result of this work.

II. MODELS AND SIMULATION METHOD

In our simulations we consider a system consisting of $2N$ hard spheres. Half of the particles carry a positive charge, and the other half carry a negative charge. All the ions considered in this work have unit charge (i.e., $z_i = 1$ for all i). The diameters of cations and anions are allowed to vary; these are denoted by σ_+ and σ_- , respectively. Ions interact via a hard-core and a Coulombic potential energy function given by

$$U_{ij} = \begin{cases} +\infty & r_{ij} \leq \sigma_{ij} \\ \frac{e^2}{4\pi\epsilon_0} \frac{z_i z_j}{r_{ij}} & r_{ij} > \sigma_{ij} \end{cases}, \quad (1)$$

where σ_{ij} is the collision diameter between ions i and j , given by $\sigma_{ij} = (\sigma_i + \sigma_j)/2$, e is the charge of the electron ($e = 1.602 \times 10^{-19}$ C), and D_0 is the dielectric permeability of vacuum ($D_0 = 8.85 \times 10^{-12}$ C²N⁻¹m⁻²).

The focus of this work is to investigate how the ratio of diameters of cations and anions, denoted by $\lambda = \sigma_+ / \sigma_-$, influences the phase behavior of electrolytes. Throughout this paper, results are reported in reduced units. We define a mean diameter according to $\sigma_{\pm} = (\sigma_+ + \sigma_-)/2$. We then define a reduced temperature, density, and box size according to $T^* = 4\pi\epsilon_0\sigma_{\pm}^3 k_B T / e^2$, $\rho^* = 2N\sigma_{\pm}^3 / V$, and $L^* = L / \sigma_{\pm}$, respectively.

For symmetric electrolytes, the critical temperature is in the neighborhood of $T^* \approx 0.05$. Simulations of coexistence must therefore be conducted at fairly low temperatures. This complicates significantly the sampling of phase space by traditional simulation methods. One way of overcoming sampling bottlenecks is of course to conduct excessively long simulations. In that regard, it is advantageous to use as many

time-saving techniques as possible to alleviate the computational burden of such calculations. In this context, the recent work of Panagiotopoulos and Kumar¹⁰ is noteworthy in that they propose a departure from a continuum through a discretization of the RPM model into a finely spaced grid. This reduces the problem of calculating interaction energies into that of looking up interactions in a table. Unfortunately, such a discretization has the potential of introducing uncontrolled approximations which could adversely affect the accuracy of predictions for new, unexplored systems. Furthermore, the level of resolution for small and large particles (as in asymmetric electrolytes) on a single grid is necessarily different. Alternatively, one can try to improve the sampling by resorting to less traditional simulation techniques. In this work, as in our recent study of the RPM, we have opted to follow the latter route, and simulations have been conducted in the framework of the hyperparallel tempering Monte Carlo method (HPTMC).⁶

Recent studies have shown that, for complex fluids, HPTMC can improve considerably the sampling of phase space.¹¹ The details of the method have been reported elsewhere.^{6,11} For completeness, only a brief description is provided here. HPTMC relies on the construction of a composite ensemble, consisting of M noninteracting replicas of general ensembles, each at a different thermodynamic state. The partition function of those ensembles is given by

$$Z = \sum_x \Omega(x) w(x) \prod_j \exp(f_j q_j(x)), \quad (2)$$

where x denotes a microscopic state of the system, $\Omega(x)$ is the density of states, $w(x)$ is an arbitrary weighting function for state x , the f_j 's are generalized potentials, and the q_j 's are the corresponding conjugate generalized variables of the system. The partition function of the composite ensemble is given by

$$Z_c = \prod_{i=1}^M Z_i. \quad (3)$$

In order to sample the configuration space of the composite ensemble, it is now possible to devise a Monte Carlo method in which configuration "swaps" between pairs of replicas i and $i+1$ are proposed. Note that swap trial moves should be supplemented by traditional Monte Carlo moves in the relevant underlying ensembles (e.g., random particle displacements for a canonical ensemble). After a swap attempt, we would have

$$\begin{aligned} x_i^{\text{new}} &= x_{i+1}^{\text{old}}, \\ x_{i+1}^{\text{new}} &= x_i^{\text{old}}, \end{aligned} \quad (4)$$

and the proposed swap would be accepted according to

$$p_{\text{acc}}(x_i \rightarrow x_{i+1}) = \min \left[1, \frac{w_i(x_{i+1}) w_{i+1}(x_i)}{w_i(x_i) w_{i+1}(x_{i+1})} \times \prod_j \exp(-\Delta f_j \Delta q_j) \right], \quad (5)$$

where $\Delta f_j = f_{j,i+1} - f_{j,i}$ is the difference in generalized potentials f_j between the two replicas, and Δq_j is the difference in the corresponding conjugate generalized variables.

TABLE I. Effect of λ on apparent critical parameters for size-asymmetric electrolytes.

λ	L^*	T_c^*	ρ_c^*
1	17	0.0492(2)	0.073(2)
0.75	17	0.0488(2)	0.072(2)
0.50	18	0.0475(3)	0.070(2)
0.25	18	0.0422(3)	0.059(3)
0.20	20	0.0386(4)	0.051(3)
0.10	22	0.0297(5)	0.033(4)
0.05	28	0.0263(6)	0.022(3)

In the particular implementation of HPTMC employed here, a replica i (or simulation box) represents a grand canonical ensemble at specified values of μ_i , V , and T_i . Ions are inserted or removed in pairs, so that electrical neutrality is preserved. To facilitate particle insertions, distance-biased methods⁷ are also implemented. For an underlying grand canonical ensemble, the acceptance criteria for swap trial moves is given by

$$p_{\text{acc}}(x_i \rightarrow x_{i+1}) = \min[1, \exp(\Delta\beta\Delta U - \Delta(\beta\mu)\Delta N)], \quad (6)$$

where $\Delta\beta = \beta_{i+1} - \beta_i$, $\Delta U = U(x_{i+1}) - U(x_i)$, $\Delta(\beta\mu) = \beta_{i+1}\mu_{i+1} - \beta_i\mu_i$, and $\Delta N = N(x_{i+1}) - N(x_i)$.

In most of our calculations we employ between 10 and 15 replicas. The composite system is simulated in parallel for at least 2×10^6 Monte Carlo steps to calculate a coexistence curve. Each Monte Carlo step consists of 200 particle displacements, 100 insertion or deletion attempts. Configuration swaps are attempted every 20 Monte Carlo steps. Instantaneous numbers of particles and total potential energy are stored every 10 Monte Carlo steps. To estimate critical properties, 4 or 5 boxes are simulated in parallel for at least 10×10^6 Monte Carlo steps. Longer simulations are required as the asymmetry of the ions increases. The box sizes employed in this work are reported in Table I.

As in our previous work, long-range interactions are calculated by the Ewald-sum method, with conducting boundary conditions. Joint histograms are collected for the distribution of number of particles and total potential energy of each simulation box. Histogram reweighting techniques^{12,13} are then used to blend histograms and to generate binodal curves. Apparent critical parameters for a given box size are estimated by means of mixed-field finite-size scaling techniques^{14,15} assuming that the criticality of the systems investigated here belongs to the Ising universality class.

III. RESULTS AND DISCUSSION

Figure 1 shows simulated binodal curves for asymmetric ionic systems. For clarity, coexistence curves are only shown for $\lambda=1, 0.75, 0.50$, and 0.25 . The corresponding critical temperatures and critical densities are reported in Table I. The sizes of the simulation boxes employed are also given in Table I. The results of our simulations indicate that as λ decreases from 1 (the restricted model) to 0.05 (the most asymmetric system considered here), both T_c^* and ρ_c^* decrease. The drop of T_c^* becomes increasingly apparent as λ becomes smaller. For nearly symmetric electrolytes (e.g., $\lambda=0.75$), the effect of λ is relatively small. The binodal

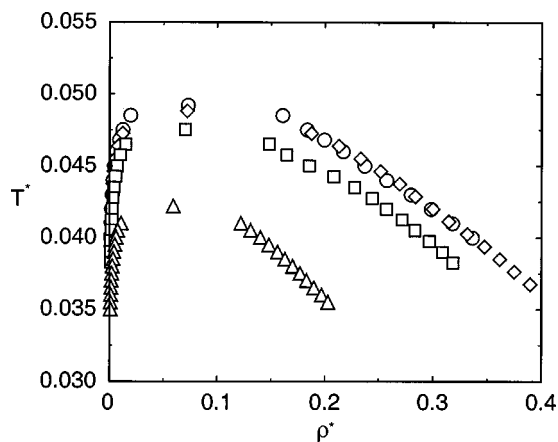


FIG. 1. Simulated binodal curves for size-asymmetric electrolyte systems with different λ . Circles: $\lambda=1$; diamonds: $\lambda=0.75$; squares: $\lambda=0.5$; triangles: $\lambda=0.25$.

curves corresponding to $\lambda=1$ and $\lambda=0.75$ are almost identical. For highly asymmetric systems, the effect of λ is much stronger and the coexistence curves show pronounced differences.

The trends of T_c^* and ρ_c^* with size asymmetry observed in simulations can now be compared to existing theoretical

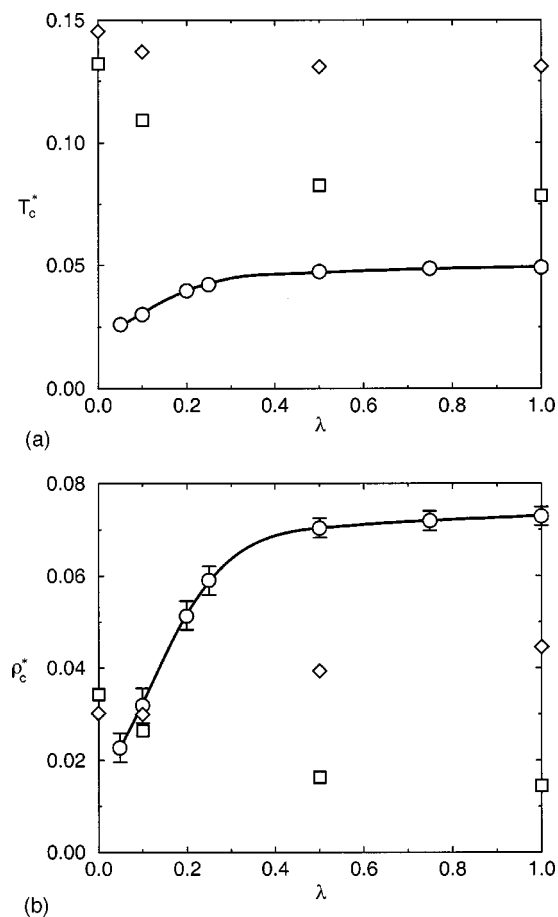


FIG. 2. Critical parameters for size-asymmetric PM electrolytes. (a) Critical temperature as a function of asymmetry. Circles correspond to results of simulations; squares are MSA results via the energy route, and diamonds are MSA results via the virial route. (b) Critical density as a function of asymmetry. The meaning of the symbols is the same as in (a).

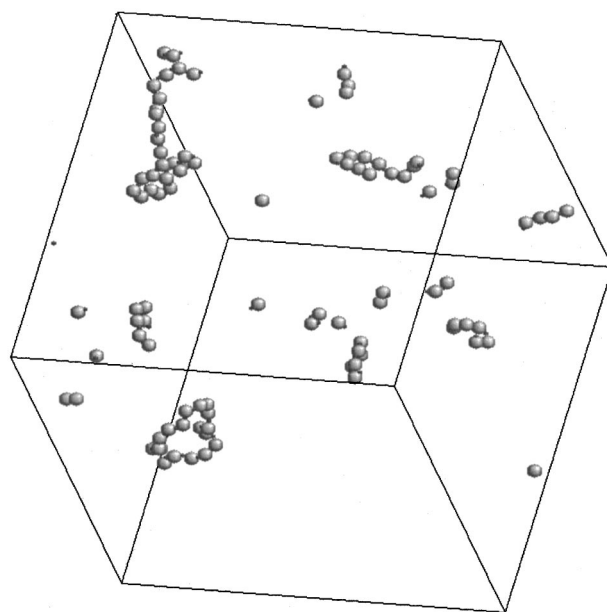


FIG. 3. Configuration representative of size-asymmetric ionic system with $\lambda=0.1$ and $L^*=55$ at $T^*=0.03$. The instantaneous density corresponding to this configuration is $\rho^*=0.00122$.

predictions. Note that until now, theory provided the only means for studying the phase behavior of asymmetric electrolytes. Figure 2 shows results from integral equation calculations using a mean spherical approximation (MSA). Predictions of MSA are shown for both the virial and the energy routes.⁹ As expected from a mean-field calculation, the MSA critical predictions are unable to capture the results of simulations quantitatively. What is perhaps more surprising, however, it that the trends predicted by the theory are in conflict with those observed in simulations. The MSA theory predicts that both the critical temperature and density *increase* as λ decreases. One possible source of this conflict is that the MSA theory does not satisfy the Debye–Hückel limiting law, which becomes important in the regime of our simulations. In a recent paper, Blum *et al.* have pointed out that this limiting law can only be satisfied by taking into account three-body interactions.¹⁶ Their new BIMSA theory, which takes three-body hard core exclusion into account, does satisfy this limiting law, and might prove to be consistent with our simulation data. Unfortunately, theoretical critical predictions using BIMSA are not available yet.

Previous authors have studied the aggregation of ions into clusters within the framework of the RPM model.¹⁷ Our results indicate that asymmetric electrolytes also form clusters, but that these are much larger than those in symmetric systems. Figure 3 shows several clusters from a simulation of the $\lambda=0.1$ system in a box of size $L^*=55$ at $T^*=0.03$. The instantaneous density is $\rho^*=0.00122$. As can be seen in the figure, ions form polymer-like structures whose shapes include chains, rings, and branched chains. This pronounced tendency to cluster can be rationalized by considering a simple aggregate of only four ions. As shown in Fig. 4, for a symmetric electrolyte the potential energy of a tight four-ion cluster is lower than that of a linear-tetramer. For highly asymmetric systems (e.g., $\lambda<0.12$), however, linear tetram-

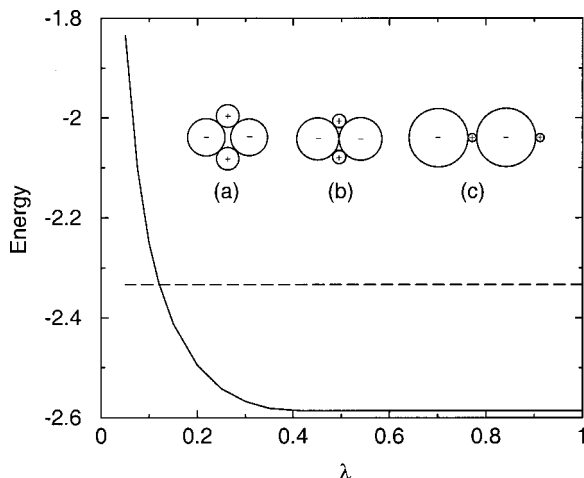


FIG. 4. Potential energy of a simple cluster of four ions at different configurations. The solid line is the calculated potential energy of compact clusters, the dashed line is that for a linear tetramer. The numerical values are in unit of $(4\pi DD_0 e^{-2}\sigma_{\pm})^{-1}$. Inserts are schematic representations of clusters: (a) compact cluster when $\lambda > \sqrt{2} - 1$; (b) compact cluster when $\lambda \leq \sqrt{2} - 1$; (c) linear cluster (tetramer).

ers have lower potential energy than any other cluster shape. This lower energy and a higher entropy help explain why chains and large rings occur. It is also interesting to point out that, for $\lambda > 0.4$, the energy of linear tetramers or clusters is independent of λ . For $\lambda < 0.4$, however, the energy of clusters increases markedly as λ decreases, while that of linear tetramers remains unchanged. Interestingly, $\lambda \approx 0.4$ is also the point at which the critical temperature and density appear to take a sharp turn towards smaller values.

To analyze this phenomenon, ions are labeled as belonging to a cluster if the smallest distance between the ion and the other members of the cluster is less than some critical distance R_c .¹⁸ For particle pair ij , in this work the critical distance is set to $R_{ij,c} = 1.5\sigma_{ij}$. Figure 5 shows the fraction of ions involved in clusters of a given size n , for $\lambda=0.1$, at $T^*=0.03$ and $\langle \rho^* \rangle = 0.003$ (for comparison, we also show results for the RPM model at a similar density.) As expected,

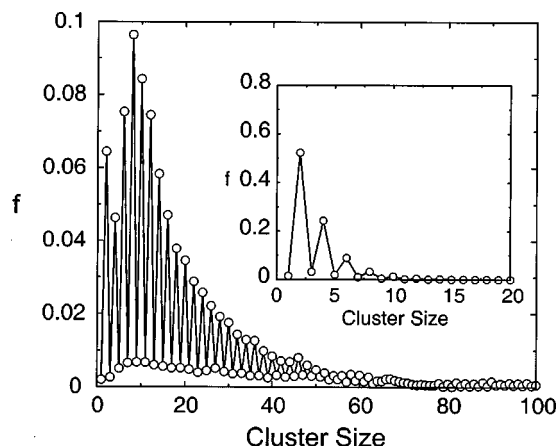


FIG. 5. Probability of finding an ion involved in a cluster of size n at $T^* = 0.03$ and $\rho^* = 0.003$ for a $\lambda = 0.1$ system of size $L^* = 91$. The insert is the same plot for RPM at $T^* = 0.051$ and $\rho^* = 0.002$ in a system of size $L^* = 50$.

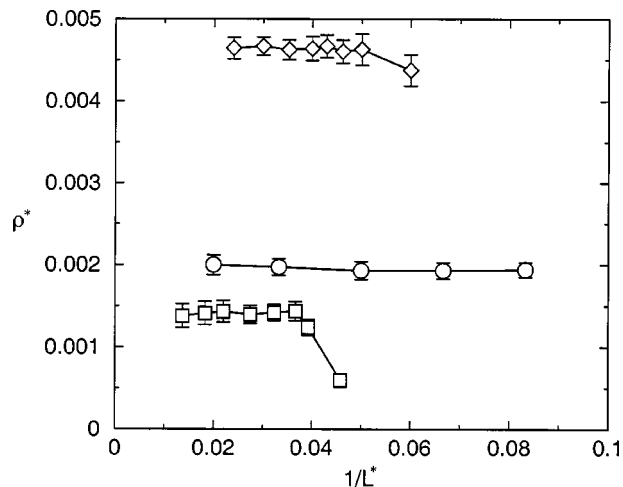


FIG. 6. Average density as a function of inverse box size. Squares: $\lambda=0.1$ at $T^*=0.03$ and $\beta\mu=-69.8$; circles: $\lambda=1$ at $T^*=0.051$ and $\beta\mu=-27$; diamonds: $\lambda=0.2$ at $T^*=0.042$ and $\beta\mu=-28$.

most clusters are neutral. The cluster size distribution exhibits an interesting maximum at $n=8$, indicating that at this density and temperature ions are more likely to be part of an octamer than a dimer; furthermore, our analysis suggests that most clusters are in chain-like structures, which can comprise as many as 100 ions. For symmetric systems at approximately the same density, most of the ions associate into pairs and most of the clusters involve less than ten ions. As shown in this work, this strong tendency of asymmetric systems to associate influences the thermodynamic properties of primitive models. It is also likely to have important effects on the transport properties of electrolyte solutions; it would be interesting to explore such properties in the future and consider how clustering affects viscosity, diffusion, etc.

The formation of large clusters in highly asymmetric electrolytes suggests that finite-size effects, analogous to those encountered in simulations of polymers, are likely to be large. To assess the magnitude of such effects, we have conducted a number of simulations in boxes of different sizes, under the same conditions of temperature and chemical potential. As Fig. 6 illustrates, for the symmetric RPM, all box sizes investigated here result in the same average density. In contrast, for a highly asymmetric PM ($\lambda=0.1$), the average density obtained for different box sizes varies considerably. For small and intermediate box sizes, the simulated average density increases until the system size reaches some critical value, after which the density keeps nearly constant. Note that for highly asymmetric electrolytes, the "critical" box size required to reduce systematic finite-size effects is large (for $\lambda=0.1$, this value is around 24). While we have verified that our systems and calculations are large enough not to be adversely affected by finite-size effects, it is important to emphasize that, at low temperatures and concentrations (i.e., for highly asymmetric systems), finite-size effects become increasingly pronounced. It would therefore be difficult to conduct simulations of coexistence below the range of λ considered in this work (that is, $\lambda < 0.05$). Also note that, to the best of our knowledge, the simulations reported here have been conducted on systems larger than

those considered by other simulation studies.^{7,8,17,19} We hope that the results presented here will prompt researchers with more developed computational muscles to go beyond the size asymmetries considered here.

Note added in proof: After completion of this work, we received a preprint of Ref. 20 describing simulations for size-asymmetric electrolytes by fine-discretization Monte Carlo method. Critical temperatures and densities are in agreement with results from this work, within statistical uncertainties.

ACKNOWLEDGMENT

Financial support from the National Science Foundation (CTS9901430) is gratefully acknowledged.

¹P. W. Debye and E. Hückel, Phys. Z. **24**, 185 (1923).

²L. Belloni, Chem. Phys. **99**, 43 (1985).

³L. Belloni, Phys. Rev. Lett. **57**, 2026 (1986).

⁴A. K. Sabir, L. B. Bhuiyan, and C. W. Outhwaite, Mol. Phys. **93**, 1273 (1994).

⁵F. O. Raineri, J. P. Routh, and G. Stell, J. Phys. IV **10**, 99 (2000).

⁶Q. Yan and J. J. de Pablo, J. Chem. Phys. **111**, 9509 (1999).

⁷F. O. Orkoulas and A. Z. Panagiotopoulos, J. Chem. Phys. **110**, 1581 (1999).

⁸J. M. Caillol, D. Levesque, and J. J. Weis, J. Chem. Phys. **107**, 1565 (1997).

⁹E. González-Tovar, Mol. Phys. **97**, 1203 (1999).

¹⁰A. Z. Panagiotopoulos and S. K. Kumar, Phys. Rev. Lett. **83**, 2981 (1999).

¹¹Q. Yan and J. J. de Pablo, J. Chem. Phys. **113**, 1276 (2000).

¹²A. M. Ferrenberg and R. H. Swendsen, Phys. Rev. Lett. **61**, 2635 (1988).

¹³A. M. Ferrenberg and R. H. Swendsen, Phys. Rev. Lett. **63**, 1195 (1989).

¹⁴A. D. Bruce and N. B. Wilding, Phys. Rev. Lett. **68**, 193 (1992).

¹⁵N. B. Wilding and A. D. Bruce, J. Phys.: Condens. Matter **4**, 3087 (1992).

¹⁶O. Bernard and L. Blum, J. Chem. Phys. **112**, 7227 (2000).

¹⁷J. M. Caillol and J. J. Weis, J. Chem. Phys. **102**, 7610 (1995).

¹⁸M. J. Gillan, Mol. Phys. **49**, 421 (1983).

¹⁹F. O. Orkoulas and A. Z. Panagiotopoulos, J. Chem. Phys. **101**, 1452 (1994).

²⁰J. M. Romero-Enrique, G. Orkoulas, A. Z. Panagiotopoulos, and M. E. Fisher, Phys. Rev. Lett. **85**, 4558 (2000).